A Novel Current Sharing Method by Grouping Transformer's Secondary Windings for a Multiphase LLC Resonant Converter

Yugang Yang, *Senior Member, IEEE*, Junyou Yao, Heng Li, and Jinsheng Zhao

***Abstract*—A novel current sharing method for a multiphase LLC resonant converter is proposed in this article. Without additional components or control strategies, the proposed method can achieve good current sharing performance even with 10% tolerance of the resonant parameters. Besides, the proposed method is very simple; only the secondary windings of the transformers need to be grouped. This method does not affect the efficiency and load transient characteristics of the LLC resonant converter. The excellent current sharing capability of the proposed method is demonstrated via theoretical analysis under first harmonic approximation assumption and powersim simulation. The experimental results of a 960-W two-phase LLC resonant converter prototype are provided to verify the effectiveness of the proposed method.**

***Index Terms*—Current sharing method, grouping secondary windings, multiphase LLC resonant converter, resonant transformer.**

I. Introduction

NOWADAYS, the LLC resonant converter is widely applied in isolated dc/dc power conversion systems for its natural characteristics of the zero-voltage switching of primary switches and zero-current switching of secondary diodes over entire load ranges, which features high efficiency, simple structure, and easy control method [1]–[4]. In high power applications, multiphase LLC structures are required to reduce the current stresses and power losses of switch components [5], [6]. In multiphase converters, the load current must be evenly distributed among converter modules to ensure reliable operation [7]. However, the gain of the LLC resonant converter is very sensitive to resonant component parameters, whereas inevitable component parameter tolerances in practice can result in unbalanced currents among phases [8]. These unbalanced currents could lead to severe instability during operation, which, in turn, influences the efficiency and security of the system; therefore, implementation of current sharing plays a vital role in the multiphase operation of the LLC resonant converter.

To solve the current sharing issue, various methods have been proposed, among which frequency control and phase shift control, as well as active control and automatic current sharing, are the main current sharing methods.

Frequency control and phase shift control methods [9]–[12] achieve current sharing by regulating switching frequency or phase shift angle of each phase according to the load current. However, the downsides are also obvious. First, the existence of feedback mechanisms requires additional sensing circuits, which increase complexity of the whole converter system. Second, control strategies are usually complex, thereby making the stability and transient issue hard to deal with.

Active control methods employ additional switch-controlled capacitor or switch-controlled inductor to compensate resonant component parameter mismatch, which is equivalent to regulating resonant frequency according to phase current [13], [14]. Although active control methods can achieve excellent current sharing performance, this type of methods presents similar drawbacks of frequency control and phase shift control methods.

The automatic current sharing method can be appealing as it offers current sharing solutions with no extra components or control strategies. Several automatic current sharing methods have been proposed. In [15], a series input structure is proposed, in which the current sharing performance is improved at a low cost. However, it does not apply to system-level modular designs since the input voltage per phase decreases as the number of modules increases. Moreover, the gate drive circuit of the top phase is complicated [16]. In [16]–[19], some commonly used capacitor and inductor structures are proposed, whose current sharing is realized without additional components or control methods and can be easily expanded to multiphase application. However, the load current sharing performance is not as good as resonant current sharing performance [20]. A current sharing method using "EIE" shape coupling resonant inductor is proposed in [21], which exhibits an effective current sharing character. Nevertheless, this method is hard to implement in more than two phase conditions. Another way of automatic current sharing is to modify the transformer winding connection structure [22]–[24]. In [22], the transformers are series connected on the primary side and parallel connected on the secondary side. The series connection on the primary sides forces the currents on the secondary sides to be the same. However, the current stresses

Manuscript received February 16, 2019; revised May 16, 2019 and August 12, 2019; accepted September 22, 2019. Date of publication September 30, 2019; date of current version February 11, 2020. This work was supported by the National Natural Science Foundation of China under Grant U1510128 and by the Fundamental Research Program of Liaoning Province Education Department Key Lab of China under Grant LZ2015045. Recommended for publication by Associate Editor Alireza Safaee. *(Corresponding author: Yugang Yang.)*

The authors are with the Faculty of Electrical and Control Engineering, Liaoning Technical University, Huludao 125105, China (e-mail: yangyugang21@126.com; 306029174@qq.com; 1259889606@qq.com; 1262517923@qq.com).

Color versions of one or more of the figures in this article are available online at http://ieeexplore.ieee.org.

Digital Object Identifier 10.1109/TPEL.2019.2944835

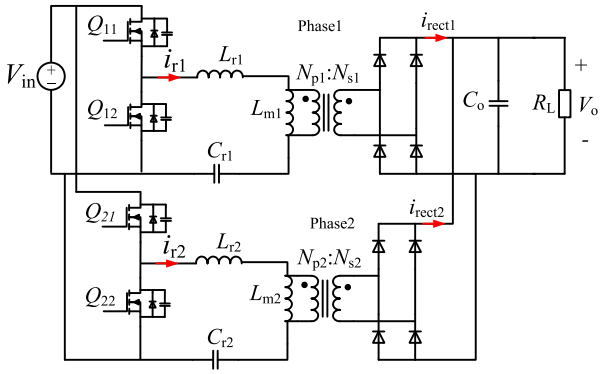

Fig. 1. Conventional two-phase LLC resonant converter.

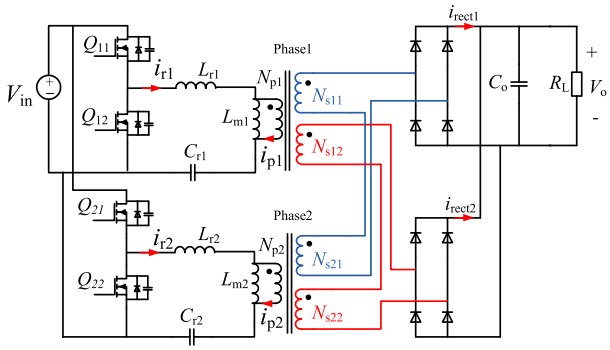

Fig. 2. Proposed two-phase LLC resonant converter.

on the primary side cannot be reduced. In [23], a parallel-series form of transformer connection is presented. On the contrary of [22], the currents of the transformer primary sides are forced to be the same by the secondary series connection, and the current stresses on the secondary sides are also not alleviated. In [24], two parallel resonant converter cells are combined by operating in interleaved half switching cycles, grouping the secondary windings and then connected them in series. This method can not only balance the primary side currents but also reduce current stresses and current ripple on the secondary side. However, this method is not easy to extend to multiphase applications.

In this article, a new current sharing method by grouping transformer's secondary windings is proposed. The transformer's secondary windings of each phase are equally divided into several branches of the same number of phases. Operating principle shows that the proposed multiphase LLC resonant converter can achieve current sharing performance automatically. In general, with no additional cost or complex control, this method is easy to implement and can be easily expanded to multiphase applications. The operating principle analysis and theoretical calculation of the current sharing error are performed in Section II. Section III presents simulation results to demonstrate the current sharing performance. Section IV provides the experimental results of a two-phase 960 W LLC resonant converter prototype applying the proposed current sharing method. Finally, the article is concluded in Section V.

II. Current Sharing Characteristic of the Proposed Multiphase LLC Resonant Converter

Fig. 1 shows the conventional two-phase LLC resonant converter, which is very sensitive to the resonant component parameters.

Based on the conventional structure, the secondary windings' connection structure is regrouped to form the proposed structure, as shown in Fig. 2.

In the proposed two-phase LLC resonant converter, the secondary windings N_{s1}, N_{s2} of the transformers as shown in Fig. 1 are respectively divided into two identical windings N_{s11}, N_{s12} and N_{s21}, N_{s22}. Windings N_{s11} of phase1 and N_{s21} of phase2 are connected in series and then connected to rectifier circuit of phase1. Symmetrically, windings N_{s12} of phase1 and N_{s22} of phase2 are connected in series and then connected to rectifier circuit of phase2.

In the cases of more than two phases, the structures are built in the same way. For example, in the three-phase situation, each phase's secondary winding is divided into three windings.

A. Basic Current Sharing Principle of the Proposed Multiphase LLC Resonant Converter

This section presents an overview of the basic current sharing principle of the proposed method. There are some assumptions as follows.

1) The windings N_{s11} and N_{s12} are winded together, and the windings N_{s21} and N_{s22} are winded together as well. They are fully coupled and have the same coupling factor with primary windings N_{p1} and N_{p2}.
2) The asymmetries of secondary sides can be ignored (the secondary PCB trace of each phase is symmetric, the rectifier diodes are ideal components) among each phase.

First, as mentioned above, the windings N_{s11} and N_{s12} are fully coupled, and the asymmetries of secondary parameters are ignored, so the current and voltage of winding N_{s11} and N_{s21} are equal to winding N_{s12} and N_{s22}, respectively. Meanwhile, for the windings N_{s11} and N_{s21} are connected in series, their currents are identical. Accordingly, the currents in the windings N_{s12} and N_{s22} are also the same. Thus, the current i_{p1} equals to current i_{p2}. As a result, since the resonant currents i_{r1} and i_{r2} are mainly determined by the currents i_{p1} and i_{p2}, respectively, the resonant currents i_{r1} and i_{r2} are almost equal with little impact of the resonant capacitors and inductors parameter errors. The analysis of the basic scheme of the proposed current sharing method in this section is based on the above assumptions. However, these assumptions would not always be valid in practical situations. The impacts of secondary asymmetries are further considered in Section B.

B. Current Sharing Performance of the Proposed Multiphase LLC Resonant Converter

This section takes two-phase as an example to analyze the current sharing characteristics of the proposed LLC resonant converter.

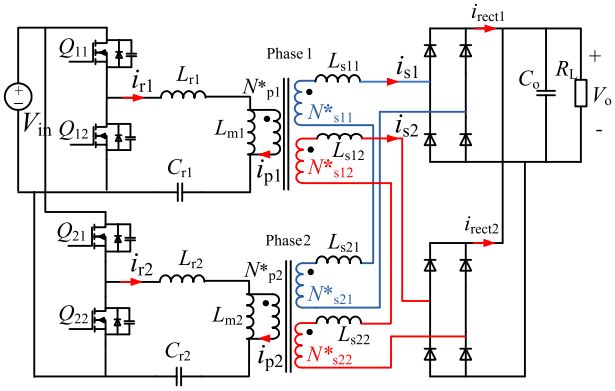

Fig. 3. Improved analytic circuit mode of the proposed LLC resonant converter.

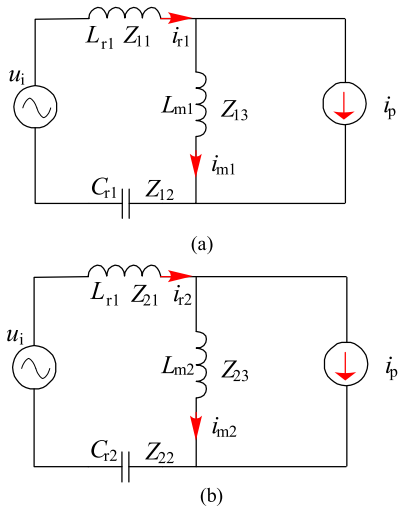

Fig. 4. (a) and (b) equivalent FHA models of the primary side.

In Section A, the secondary windings N_{s11} and N_{s12} (N_{s21} and N_{s22}) are assumed to be fully coupled, and the asymmetries between each secondary side are ignored. However, in realistic situation, even if the secondary windings of the transformer in each phase are twisted wires, there are still asymmetries between them. This section will discuss the current sharing characteristics of the proposed structure considering the asymmetries in secondary windings.

Fig. 3 shows the improved analytic circuit model, compared with the simplified circuit in Fig. 2, the leakage inductances L_{s11}, L_{s12}, L_{s21}, L_{s22} in transformer secondary sides are taken into account, and the leakage inductances on primary sides are included in resonant inductances L_{r1} and L_{r2}, respectively. The current sharing characteristics of proposed method are analyzed as follows.

1) Define Current Sharing Error's Calculation Method: The load current sharing error δI_o and resonant current sharing error δi_r are defined respectively in (1) and (2), where $i_{\mathrm{rect1(avg)}}$ and $i_{\mathrm{rect2(avg)}}$ are the average rectifier currents of phase1 and phase2, they are also the dc output currents of phase1 and phase2. $i_{r1(rms)}$ and $i_{r2(rms)}$ are root mean square values of resonant currents of phase1 and phase2. $\delta I_o = 0$ means that the load current has been equally shared, $\delta I_o = 1$ indicates that only one phase provides power to load

$$\delta I_o = \left| \frac{i_{\mathrm{rect1(avg)}} - i_{\mathrm{rect2(avg)}}}{i_{\mathrm{rect1(avg)}} + i_{\mathrm{rect2(avg)}}} \right| \times 100\% \tag{1}$$

$$\delta i_r = \left| \frac{i_{r1(\mathrm{rms})} - i_{r2(\mathrm{rms})}}{i_{r1(\mathrm{rms})} + i_{r2(\mathrm{rms})}} \right| \times 100\%. \tag{2}$$

2) Resonant Current Sharing Performance Analysis: As shown in Fig. 3, since leakage inductances are taken into consideration, N^*_{p1}, N^*_{s11}, and N^*_{s12} can be regarded as ideal transformer windings, as well as N^*_{p2}, N^*_{s21}, and N^*_{s22}. The relationship between current i_{p1} and i_{p2} can be derived as (3), where n is transformer turns ratio ($n = N_{p1} : N_{s11} = N_{p1} : N_{s12} = N_{p2} : N_{s21} = N_{p2} : N_{s22}$). Equation (3) shows that i_{p1} always equals to i_{p2} even when the secondary sides are asymmetrical. This feature contributes the proposed structure to achieve current sharing

$$\left.\begin{aligned} i_{p1} &= \frac{i_{s1} + i_{s2}}{n} \\ i_{p2} &= \frac{i_{s1} + i_{s2}}{n} \end{aligned}\right\} \Rightarrow i_{p1} = i_{p2} = i_p. \tag{3}$$

Fig. 4(a) and (b) shows the equivalent FHA models of the primary side of phase1 and phase2. Z_{11}, Z_{12}, Z_{13}, Z_{21}, Z_{22}, and Z_{23} are the impedances of L_{r1}, C_{r1}, L_{m1} and L_{r2}, C_{r2}, and L_{m2}, respectively, while i_{r1} and i_{r2} are amplitude values of resonant currents in phase1 and phase2.

To analyze the current sharing error between each phase, the parameters of phase1 are assigned as the references, and a certain tolerance is set to the parameters of phase2 based on the reference. Namely, L_{r2}, C_{r2}, and L_{m2} have tolerances based on references L_{r1}, C_{r1}, L_{m1}, and Z_{21}, Z_{22}, and Z_{23} have tolerances based on Z_{11}, Z_{12}, and Z_{13} respectively. And i_{r2} has error based on i_{r1} correspondingly.

According to the FHA equivalent circuit Fig. 4(a), the reference current i_{r1} can be expressed as (4)

$$i_{r1} = \frac{u_i + Z_{13} i_p}{Z_{11} + Z_{12} + Z_{13}}. \tag{4}$$

Due to the component tolerances, there is deviation of i_{r2} from i_{r1}, which is represented as di_{r21}. Thus, the relationship of resonant currents can be described as (5)

$$i_{r2} = i_{r1} + di_{r21} \tag{5}$$

According to (4), di_{r21} can be obtained as (6) by taking a partial derivative with respected to Z_{11}, Z_{12}, and Z_{13}. This means that if Z_{21}, Z_{22}, and Z_{23} deviate from Z_{11}, Z_{12}, and Z_{13}, then i_{r2} will deviate from i_{r1}, whereas both i_p and u_i have no deviation between phase1 and phase2

$$di_{r21} = \frac{-(u_i + Z_{13} i_p) dZ_{11}}{(Z_{11} + Z_{12} + Z_{13})^2} + \frac{-(u_i + Z_{13} i_p) dZ_{12}}{(Z_{11} + Z_{12} + Z_{13})^2} + \frac{[(Z_{11} + Z_{12}) i_p - u_i]\, dZ_{13}}{(Z_{11} + Z_{12} + Z_{13})^2} \tag{6}$$

The impedances Z_{11}, Z_{11}, and Z_{13} can be calculated as (7), where f_s is the switching frequency

$$\begin{cases} Z_{11} = j2\pi f_s L_{r1} \\ Z_{12} = -j\dfrac{1}{2\pi f_s C_{r1}} \\ Z_{13} = j2\pi f_s L_{m1}. \end{cases} \tag{7}$$

The impedance deviations dZ_{11}, dZ_{12}, and dZ_{13} can be calculated as (8)

$$\begin{cases} dZ_{11} = j2\pi f_s (L_{r2} - L_{r1}) \\ dZ_{12} = j\left(\frac{1}{2\pi f_s C_{r1}} - \frac{1}{2\pi f_s C_{r2}}\right) \\ dZ_{13} = j2\pi f_s (L_{m2} - L_{m1}). \end{cases} \tag{8}$$

Voltage u_i is the fundamental harmonic amplitude value of the resonant tank input voltage and i_p is the fundamental harmonic amplitude of N_{p1}^* (N_{p2}^*), which can be obtained as (9) according to the FHA analysis, where I_o is the output load current and V_{in} is the input voltage

$$\begin{cases} i_p = \dfrac{\pi}{2n} I_o \\ u_i = \dfrac{2}{\pi} V_{\text{in}}. \end{cases} \tag{9}$$

The format of the resonant current sharing error defined in (2) can be modified to (10) so as to utilize (6) for further derivation

$$\begin{aligned} \delta i_r &= \left| \frac{i_{r1(\text{rms})} - i_{r2(\text{rms})}}{i_{r1(\text{rms})} + i_{r2(\text{rms})}} \right| \times 100\% \\ &= \left| \frac{(i_{r1} + di_{r21}) - i_{r1}}{(i_{r1} + di_{r21}) + i_{r1}} \right| \times 100\% = \left| \frac{\frac{di_{r21}}{i_{r1}}}{\frac{di_{r21}}{i_{r1}} + 2} \right| \times 100\%. \end{aligned} \tag{10}$$

Combining (4), (6), and (10), the resonant current sharing error can be calculated as (11)

$$\delta i_r = \frac{\left| dZ_{11} + dZ_{12} + dZ_{13} \left| \frac{(Z_{11}+Z_{12})i_p - u_i}{Z_{13} i_p + u_i} \right| \right|}{\left| \left(dZ_{11} + dZ_{12} + dZ_{13} \left| \frac{(Z_{11}+Z_{12})i_p - u_i}{Z_{13} i_p + u_i} \right| \right) + 2(Z_{11} + Z_{12} + Z_{13}) \right|}. \tag{11}$$

Equation (11) shows that the resonant current sharing error is related to u_i, i_p and component impedance deviations, but independent of the asymmetries of the secondary sides.

As Z_{11}, Z_{13} are inductive impedances and Z_{12} is capacitive impedance, $Z_{11} + Z_{12} + Z_{13}$ normally exhibits an inductive impedance characteristic within a full switching frequency range of the LLC resonant converter, thereby $Z_{11} + Z_{12} + Z_{13} > 0$. Besides, L_{m1} is larger than L_{r1} (normally $L_{m1} > 2\,L_{r1}$ at least), so $Z_{13} > 2Z_{11}$. Therefore, inequality (12) is can be derived as

$$|Z_{11} + Z_{12}| < |Z_{13}| \Rightarrow \left| \frac{(Z_{11} + Z_{12})i_p - u_i}{Z_{13} i_p + u_i} \right| < 1. \tag{12}$$

Hence, the resonant current sharing error is in accordance with (13) shown at the bottom of the next page.

Considering dZ_{11}, dZ_{12}, and dZ_{13} are much smaller than Z_{11}, Z_{12}, and Z_{13} respectively, and $Z_{13} > 2Z_{12}$, $Z_{11} + Z_{12} + Z_{13} > 0$, for a simple estimate in the worst case, the resonant current sharing error can be approximated by (14). For example, if $L_{r2} = (1 + 10\%)L_{r1}$, $C_{r2} = (1 + 10\%)C_{r1}$, $L_{m2} = (1 + 10\%)L_{m1}$, the resonant current sharing error δi_r is no more than 15% by simple estimate, while the actual error obtained from concrete calculation is smaller than this. This reflects the current sharing capability of the proposed method

$$\delta i_r \le \left(\left| \frac{dZ_{11}}{2Z_{11}} \right| + \left| \frac{dZ_{12}}{2Z_{12}} \right| + \left| \frac{dZ_{13}}{2Z_{13}} \right| \right) \times 100\% \tag{14}$$

As shown below, to describe the theoretical resonant current sharing error of the proposed structure, the resonant current sharing error curves in relation to switching frequency under different input voltage and output load are plotted according to (11).

The nominal parameters of L_{r1} is 38.4 uH, C_{r1} is 66 nF, and $L_{m1} = 153.6$ uH. The input voltage range varies from 340 to 400 V. The output voltage is 48 V, and the full load current is 20 A. The nominal parameters are assigned to phase1 as references, and parameters in phase2 have a 10% tolerance. The error curves are plotted according to the following four different tolerance combinations of phase2.

Combination1: $L_{r2} = 1.1L_{r1}$, $C_{r2} = 1.1C_{r1}$, $L_{m2} = 1.1L_{m1}$;
Combination2: $L_{r2} = 0.9L_{r1}$, $C_{r2} = 1.1C_{r1}$, $L_{m2} = 1.1L_{m1}$;
Combination3: $L_{r2} = 1.1L_{r1}$, $C_{r2} = 0.9C_{r1}$, $L_{m2} = 1.1L_{m1}$;
Combination4: $L_{r2} = 1.1L_{r1}$, $C_{r2} = 1.1C_{r1}$, $L_{m2} = 0.9L_{m1}$;

Fig. 5(a)–(d) shows the theoretical resonant current sharing error curves versus switching frequency against different parameter tolerances, among which combination 1 is obviously the worst case.

Fig. 5(a) presents the resonant current sharing error at a switching frequency from 70 to 120 kHz. It is noted that the actual working frequency is related to the input voltage and output current. The smaller the output current, the higher the switching frequency, for example, under the condition of 2 A load and 400 V input, the switching frequency is 101.7 kHz rather than 70 kHz, so the theoretical current sharing error is 4.6%, instead of 10.4%. While at 20 A load and 340 V input, the switching frequency is 77.5 kHz (according to the simulation in Section III), and the current sharing error is 7.0%.

The actual theoretical resonant current sharing errors under various input and output conditions with the four types of tolerances is presented in Section III for comparison between the theoretical calculation results and the simulation results, where the simulation switching frequency is fixed.

3) Rectifier Current Sharing Error Analysis: This section analyzes the rectifier current sharing performance. Fig. 6 shows the analytical FHA circuit models of secondary sides. As discussed above, N_{s11}^*, N_{s12}^* are the secondary windings of ideal transformer 1 in Fig. 3, while N_{s21}^*, N_{s22}^* are secondary windings of ideal transformer 2 in Fig. 3. Both the transformers are ideal units, $u_{11} = u_{12}$, $u_{21} = u_{22}$.

According to the FHA circuit models, the secondary currents can be derived as (15), where $Z_{s1} = R_{\text{para1}} + \text{j}2\pi f_s(L_{s11} + L_{s21})$, $Z_{s2} = R_{\text{para2}} + \text{j}2\pi f_s(L_{s12} + L_{s22})$, R_{para1} and R_{para2} are the equivalent parasitic resistances of the secondary circuits

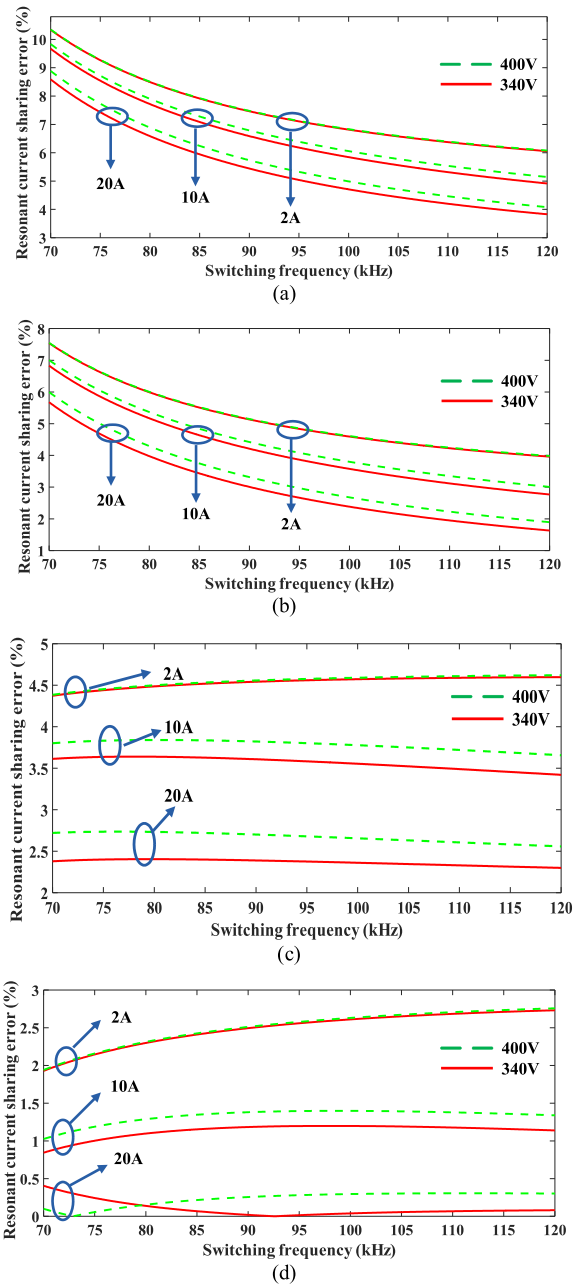

Fig. 5. Resonant current sharing error curves with respect to switching frequency with (a) tolerance combination1, (b) tolerance combination2, (c) tolerance combination3, and (d) tolerance combination4.

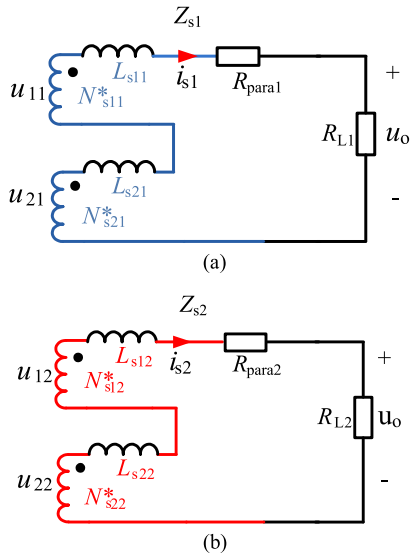

Fig. 6. (a) and (b) FHA circuit model of the secondary side.

of phase1 and phase2

$$i_{s1} = \frac{u_{11} + u_{21} - u_o}{Z_{s1}}$$
$$i_{s2} = \frac{u_{12} + u_{22} - u_o}{Z_{s2}}. \tag{15}$$

Combining (15), the rectifier current sharing error calculation expression defined in (1) can be derived as (16)

$$\delta I_o = \left| \frac{i_{\text{rect1(avg)}} - i_{\text{rect2(avg)}}}{i_{\text{rect1(avg)}} + i_{\text{rect2(avg)}}} \right| = \left| \frac{Z_{s1} - Z_{s2}}{Z_{s1} + Z_{s2}} \right| \times 100\%. \tag{16}$$

It can be seen from (16) that the rectifier current sharing error is irrelevant to the primary side.

While taking Z_{s1} as reference, Z_{s2} has a tolerance based on Z_{s1}, the rectifier current sharing error can be further obtained. Since the parasitic R_{para1} and R_{para2} are normally much smaller than the impedances of $L_{s11} + L_{s21}$ and $L_{s12} + L_{s22}$; thus, they can be ignored. Therefore, the rectifier current sharing error can be obtained as (17)

$$\delta I_o = \left| \frac{(L_{s12} + L_{s22}) - (L_{s11} + L_{s21})}{(L_{s12} + L_{s22}) + (L_{s11} + L_{s21})} \right| \times 100\%. \tag{17}$$

$$\delta i_r \le \left(\frac{|dZ_{11}|}{\left| \left(dZ_{11} + dZ_{12} + dZ_{13} \left| \frac{(Z_{11}+Z_{12})i_p - u_i}{Z_{13}i_p + u_i} \right| \right) + 2(Z_{11} + Z_{12} + Z_{13}) \right|} + \frac{|dZ_{12}|}{\left| dZ_{11} + dZ_{12} + dZ_{13} \left| \frac{(Z_{11}+Z_{12})i_p - u_i}{Z_{13}i_p + u_i} \right| + 2(Z_{11} + Z_{12} + Z_{13}) \right|} + \frac{|dZ_{13}|}{\left| dZ_{11} + dZ_{12} + dZ_{13} \left| \frac{(Z_{11}+Z_{12})i_p - u_i}{Z_{13}i_p + u_i} \right| + 2(Z_{11} + Z_{12} + Z_{13}) \right|} \right) \times 100\% \tag{13}$$

Up to this point, the current sharing characteristic of the proposed two-phase LLC resonant converter has been thoroughly analyzed. A summary for this part to further emphasize the current sharing characteristic is given as follows.

The load current sharing error is only affected by the leakage inductance imbalance on the transformer's secondary side. Therefore, according to (17), the relationship between load current sharing error and the leakage inductance imbalance on transformer secondary side can be quantitatively obtained. For example, in the condition of $L_{s12} = 1.1L_{s11}$, $L_{s22} = 1.1L_{s21}$, and $L_{s21} = 1.1L_{s11}$ (with 10% imbalance on the secondary side), the load current sharing error is 4.8%. This reflects the capacity of the proposed topology to handle the asymmetry between two transformers.

Besides, it can be seen from (11) that the resonant current sharing error is not only related to resonant inductance imbalance but also related to magnetizing inductance imbalance and resonant capacitance imbalance. Therefore, while calculating the resonant current sharing error, all these parameter imbalances should be taken into account, simultaneously. However, in order to provide an intuitive description of the impact of these imbalances, several special tolerance combinations can be assigned to resonant parameters for simple analysis as follows.

Combination A ($L_{r1} = (1 + a\%)L_{r2}$, $C_{r1} = C_{r2}$, $L_{m1} = L_{m2}$) means that only the resonant inductance imbalance is considered. Thus, (11) can be simplified as (18), and the resonant current sharing error is $0.5a\%$ approximately

$$\delta i_r = \left| \frac{dZ_{11}}{dZ_{11} + 2Z_{11}} \right| \times 100\%. \tag{18}$$

Similarly, combination B ($L_{r1} = L_{r2}$, $C_{r1} = (1 + b\%)C_{r2}$, $L_{m1} = L_{m2}$) and combination C ($L_{r1} = L_{r2}$, $C_{r1} = C_{r2}$, $L_{m1} = (1 + c\%)L_{m2}$) mean that only the resonant capacitance imbalance and magnetizing inductance imbalance are considered, respectively. With the same simplifying method, the corresponding resonant current sharing error is roughly $0.5b\%$ and $0.5c\%$, respectively.

The resonant current sharing errors caused by above tolerance combinations indicate the capability of the proposed topology to deal with the resonant inductance imbalance, resonant capacitance imbalance, and magnetizing inductance imbalance.

As mentioned, the resonant inductance includes the leakage inductance on the transformer's primary side and the extra discrete inductance that is added when the leakage inductance is not large enough for the required resonant inductance value. Hence, the analysis of combination A also presents the performance of the proposed topology structure on tolerating the transformer asymmetry. Besides, a resonant current sharing error with tolerance combination C reflects the capability of the proposed structure in handling transformer imbalance as well.

It is noted that the turn ratios of the transformers in each phase are required to be identical for the proposed structure. Actually, it is not difficult to control transformer winding number during transformer manufacturing. Therefore, this requirement is not too hard to realize.

C. Other Discussions on the Performances of the Proposed Multiphase LLC Resonant Converter

1) Phase Interleaving Capability: Generally, for the multiphase LLC converter, the current ripple in the output capacitor can be significantly reduced by adopting phase interleaving. However, the phase interleaving technique is not available for the proposed structure, since the secondary windings N_{s11} and N_{s21}, N_{s12}, and N_{s22} are connected in series, respectively. That is, the currents i_{rect1} and i_{rect2} are almost always the same, their phase angles cannot be shifted.

2) Phase Shielding Capability: The same as above, due to the series connection of the transformer secondary windings in each phase, the phase shielding capability is irrealizable in the proposed structure. That is to say, once one of the phases of the converter fails, the whole power would be lost, which is obviously a shortcoming of the proposed structure.

3) Synchronous Rectifying Capability: Because the proposed structure simply regroups the transformer's secondary windings, the rectifier working logic is the same with the conventional multiphase LLC resonant converter. The proposed structure can employ synchronous rectification technique including self-driven synchronous rectification to reach a higher efficiency.

4) Efficiency Characteristic: Compared with the conventional LLC structure, the efficiency of the proposed structure is barely affected. First of all, the current and voltage stresses across semiconductors are basically the same with the conventional ones. Besides, although the secondary windings are divided into several groups, the current in primary and secondary windings will not increase, so does the total number of coils in the transformer. Hence, the transformer size and loss are considered to remain unchanged. A comparison of efficiency tests between conventional and the proposed structure will be presented in Section IV.

5) Load Transient Performance: The proposed structure exhibits a stable load transient performance. Load transient simulation results are presented in Section III, part 3, and the test results of an experimental prototype without current control loop are presented in Section IV. Both simulation and experimental results demonstrated that the current sharing capability can still be maintained during load transients.

6) The Effect of Transformer Parasitic Capacitance: Parasitic capacitances in transformers can have a significant impact on high-frequency power electronics systems. Researchers have proposed many effective methods to mathematically analyze or experimentally extract their precise values [25]–[28]. As these papers pointed out, the amount of parasitic capacitance depends heavily on the geometry and working frequency of the transformer; thus, obtaining accurate modeling of parasitic capacitances is difficult. In this article, the proposed current sharing method is realized by dividing and regrouping the transformer secondary windings. As the quantity of transformer windings increases with the paralleled resonant converters, the parasitic capacitance effect becomes more complex and difficult to analyze than conventional transformer structures. For this reason, this article does not analyze the transformer parasitic capacitances in detail. However, even though the current sharing

TABLE I
NOMINAL PARAMETERS

Input voltage range	340~400 V
Resonant capacitors C_{r1}, C_{r2}	66 nF
Resonant inductors L_{r1}, L_{r2}	38.4 uH
Magnetizing inductors L_{m1}, L_{m2}	153.6 uH
Transformer turns ratio n	8.33(25:3:3)
Output voltage V_o	48 V
Total load power P_o	960 W

performance was not obviously affected by the transformer parasitic capacitances in the prototype experiment results shown in Section IV, further efforts are needed to study the effects of the parasitic capacitance on the proposed structure.

III. SIMULATION RESULTS ANALYSIS

This section presents the current sharing error PSIM simulation results of a conventional two-phase LLC resonant converter as shown in Fig. 1, and the proposed structure as shown in Fig. 5. Correspondingly, the theoretical calculation results of the proposed structure are presented. Moreover, a comparison of PSIM simulation results between the proposed method and the other most recent automatic current sharing methods proposed in [19] is made. Finally, the load transient simulation results of the proposed structure are presented.

Part 1: Simulation of the conventional structure and the proposed structure.

The nominal parameters are listed in Table I. The four combinations of resonant component tolerances in Section II are applied as operation conditions in simulation.

Considering the asymmetries of the secondary windings of the proposed structure, the leakage inductances L_{s11}, L_{s12}, L_{s21}, and L_{s22} are taken into account in all simulations.

While L_{s11} and L_{s21} are assigned as references, L_{s12} and L_{s22} will have tolerances based on L_{s11} and L_{s21}, respectively. Since that the values of leakage inductances L_{s11}, L_{s12}, L_{s21}, and L_{s22} in the experimental prototype are too small to be accurately measured (0.1 uH approximately), L_{s11} and L_{s21} are assigned to be 0.1 uH and 0.11 uH in simulation, which is reasonable for the simulation to verify the theoretical current sharing errors and the impacts of secondary asymmetries on current sharing performance.

#1: Compare current sharing error between conventional and proposed topology structure. $L_{r2} = 1.1L_{r1}, C_{r2} = 1.1C_{r1}$, $L_{m2} = 1.1L_{m1}$; $L_{s12} = 1.1L_{s11}$, $L_{s22} = 1.1L_{s21}$, $L_{s21} = 1.1L_{s11}$; input voltage is 340 V, output is 48 V 20 A, the simulation results are shown in Table II, and the waveforms are shown in Fig. 7(a)–(d).

Table II lists the resonant current sharing error δi_r and rectifier current sharing error (load current sharing error) δI_o, and theoretical calculation results δi_r_cal and δI_o_cal. δi_r and δI_o are 54.3% and 100% of the conventional structure, 5.6% and 4.7% of the proposed topology structure, which demonstrates the notable current sharing improvement of the proposed method. In addition, δi_r_cal is 7.0%, and δI_o_cal is 4.8%, which are basically consistent with simulation results.

Fig. 7(a) and (b) presents the resonant current and rectifier current waveforms of the conventional structure, where the

TABLE II
SIMULATION RESULTS OF THE CONVENTIONAL AND PROPOSED STRUCTURE

Result / Structure	i_{r1} (A)	i_{r2} (A)	δi_r (%)	δi_r_cal (%)
Conventional structure	6.72	1.99	54.3	-
Proposed structure	4.04	3.61	5.6	7.0
Result / Structure	i_{rect1} (A)	i_{rect2} (A)	δI_o (%)	δI_o_cal (%)
Conventional structure	20.37	0	100	-
Proposed structure	10.27	9.34	4.7	4.8

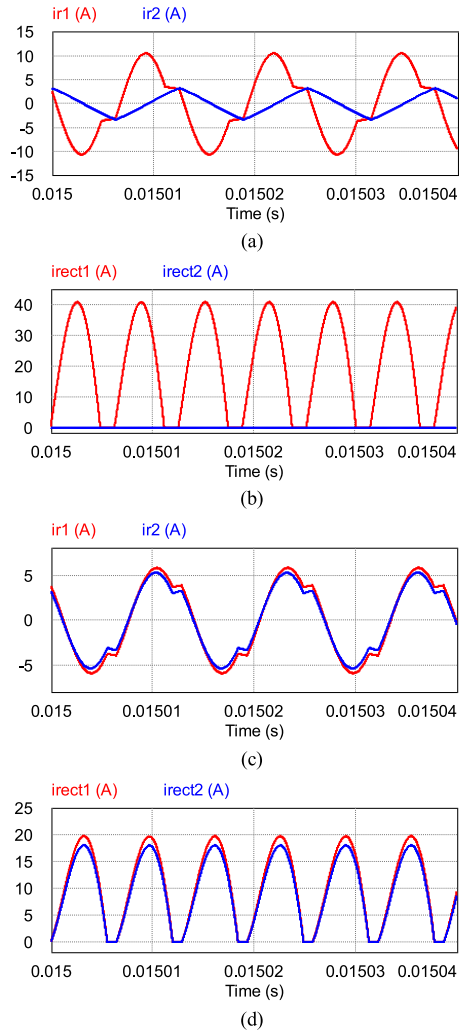

Fig. 7. Simulation waveforms with $L_{r2} = 1.1L_{r1}, C_{r2} = 1.1C_{r1}, L_{m2} = 1.1L_{m1}$; $L_{s12} = 1.1L_{s11}$, $L_{s22} = 1.1L_{s21}$, $L_{s21} = 1.1L_{s11}$: (a) and (b) conventional structure resonant current and rectifier current; (c) and (d) proposed structure resonant current and rectifier current.

TABLE III
SIMULATION RESULT OF THE PROPOSED STRUCTURE

Result / Condition	f_s kHz	i_{r1} (A)	i_{r2} (A)	δi_r (%)	δi_{r_cal} (%)
#1	77.5	4.04	3.61	5.6	7.0
#2	101.5	2.00	1.83	4.4	4.6
#3	101.7	1.99	1.83	4.2	4.6
#4	78.5	4.00	3.93	0.8	0.2
Result / Condition	f_s kHz	i_{rect1} (A)	i_{rect2} (A)	δI_o (%)	δI_{o_cal} (%)
#1	77.5	10.27	9.34	4.7	4.8
#2	101.5	1.03	0.94	4.6	4.8
#3	101.7	1.03	0.94	4.6	4.8
#4	78.5	10.27	9.34	4.7	4.8

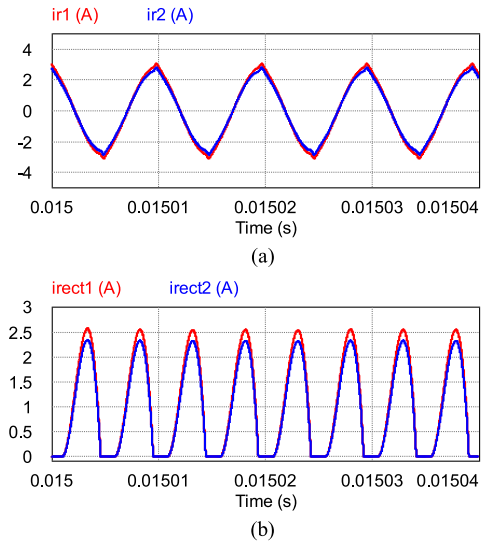

Fig. 8. Simulation waveforms with $L_{r2} = 0.9L_{r1}$, $C_{r2} = 1.1C_{r1}$, $L_{m2} = 1.1L_{m1}$; $L_{s12} = 1.1L_{s11}$, $L_{s22} = 1.1L_{s21}$, $L_{s21} = 1.1L_{s11}$: (a) and (b) proposed structure resonant current and rectifier current.

currents of phase1 and phase2 are seriously out of balance. The current sharing capability is obviously improved in the proposed structure as shown in Fig. 7(c) and (d).

#2: Compare the simulation results and theoretical calculation results of the proposed structure. $L_{r2} = 0.9L_{r1}$, $C_{r2} = 1.1C_{r1}$, $L_{m2} = 1.1L_{m1}$; $L_{s12} = 1.1L_{s11}$, $L_{s22} = 1.1L_{s21}$, $L_{s21} = 1.1L_{s11}$; input voltage is 400 V, and the output is 48 V 2 A. The simulation results are shown in Table III and Fig. 8.

#3: Compare the simulation results and theoretical calculation results of the proposed structure. $L_{r2} = 1.1L_{r1}$, $C_{r2} = 0.9C_{r1}$, $L_{m2} = 1.1L_{m1}$; $L_{s12} = 1.1L_{s11}$, $L_{s22} = 1.1L_{s21}$, $L_{s21} = 1.1L_{s11}$, input 400 V, output 48 V 2 A. The simulation results are shown in Table III and Fig. 9.

#4: Compare the simulation results and theoretical calculation results of the proposed structure. $L_{r2} = 1.1L_{r1}$, $C_{r2} = 1.1C_{r1}$, $L_{m2} = 0.9L_{m1}$; $L_{s12} = 1.1L_{s11}$, $L_{s22} = 1.1L_{s21}$, $L_{s21} = 1.1L_{s11}$; input voltage 340 V, output current 20 A. The simulation results are shown in Table III and Fig. 10.

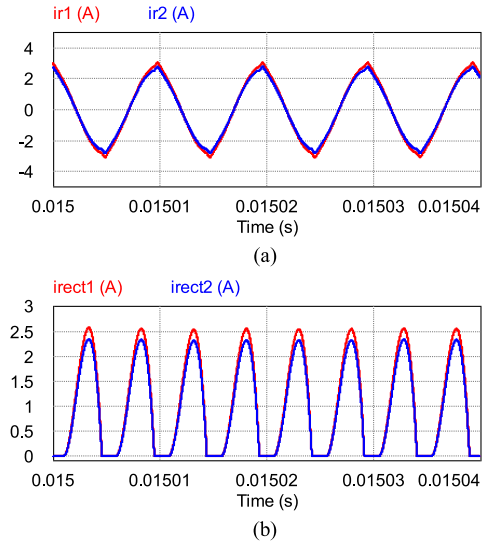

Fig. 9. Simulation waveforms with $L_{r2} = 1.1L_{r1}$, $C_{r2} = 0.9C_{r1}$, $L_{m2} = 1.1L_{m1}$; $L_{s12} = 1.1L_{s11}$, $L_{s22} = 1.1L_{s21}$, $L_{s21} = 1.1L_{s11}$: (a) (b) proposed structure resonant current and rectifier current.

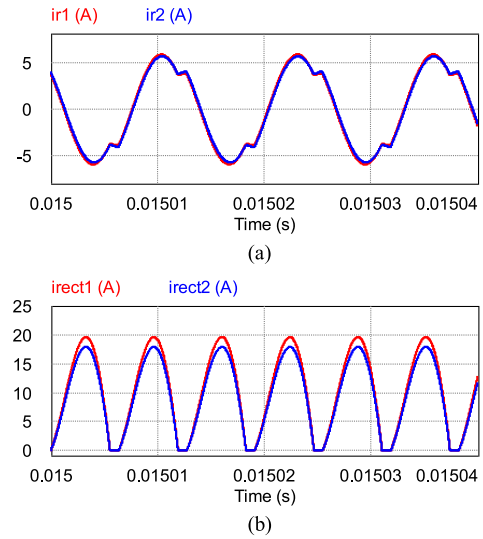

Fig. 10. Simulation waveforms with $L_{r2} = 1.1L_{r1}$, $C_{r2} = 1.1C_{r1}$, $L_{m2} = 0.9L_{m1}$; $L_{s12} = 1.1L_{s11}$, $L_{s22} = 1.1L_{s21}$, $L_{s21} = 1.1L_{s11}$: (a) and (b) proposed structure resonant current and rectifier current.

The waveforms in Figs. 7–10 are simulation currents under four different combinations of parameter tolerances. Obviously, tolerance type #1 is the worst case among the others, which is consistent with the current sharing error curve analyzed in Section II, thus validating the mathematical current sharing error formula.

The detailed simulation result data are shown in Table III. With a parameter tolerance of 10%, and combination of type1, the worst resonant current sharing error simulation is 5.6%, under the operation condition of 340 V input and 20 A load. The

TABLE IV
COMPARISON RESULT OF COMMON CAPACITOR STRUCTURE AND PROPOSED STRUCTURE WITH 5% RESONANT PARAMETER TOLERANCE

Result / Structure	i_{r1} (A)	i_{r2} (A)	δi_r (%)
Common capacitor structure	2.47	2.28	4.0
Proposed structure	3.91	3.69	2.9
Result / Structure	i_{rect1} (A)	i_{rect2} (A)	δI_o (%)
Common capacitor structure	27.83	22.20	11.3
Proposed structure	10.33	9.39	4.8

theoretical resonant current sharing error is 7.0%, having an error of 1.4% in comparison with the simulation result due to the FHA analysis inaccuracy. The calculated rectifier current sharing error is 4.8%, while the simulation rectifier current sharing errors are nearly 4.8%, which demonstrates the correctness of theoretical analysis and the excellent current sharing performance even in the case of asymmetrical secondary sides.

Part 2: Comparison between the proposed structure in this article and the *common capacitor* structure proposed in [19].

In [19], the current sharing performance of the common capacitor structure has been analyzed, where with 5% parameter tolerance, the worst case is in the $L_{r2} = 1.05L_{r1}$, $C_{r2} = 1.05C_{r1}$, and $L_{m2} = 0.95L_{m1}$ condition. However, for the proposed structure in this article, the worst case is in the condition of $L_{r2} = 1.05L_{r1}$, $C_{r2} = 1.05C_{r1}$, and $L_{m2} = 1.05L_{m1}$. This part compares the current sharing performance between the common capacitor structure and the proposed structure of this article under their respective worst tolerance combinations.

#1: Compare current sharing performance with 5% resonant component parameter tolerances. The common capacitor structure is at the $L_{r2} = 1.05L_{r1}$, $C_{r2} = 1.05C_{r1}$, $L_{m2} = 0.95L_{m1}$, 50 A full load, 400 V input condition, while the proposed structure operates at $L_{r2} = 1.05L_{r1}$, $C_{r2} = 1.05C_{r1}$, $L_{m2} = 1.05L_{m1}$, and $L_{s12} = 1.1L_{s11}$, $L_{s22} = 1.1L_{s21}$, $L_{s21} = 1.1L_{s11}$, 340 V input voltage, 20 A full load. The simulation results are given in Table IV and Fig. 11.

In simulation results of #1, the resonant current sharing error is 4.0% in the common capacitor structure and 2.9% in the proposed topology structure. The rectifier current sharing error is 11.3% in the common capacitor structure and 4.8% in the proposed structure, indicating that the proposed structure has a better performance.

#2: Compare current sharing performance with 10% parameter tolerances. The common capacitor structure is under $L_{r2} = 1.1L_{r1}$, $C_{r2} = 1.1C_{r1}$, $L_{m2} = 0.9L_{m1}$, 50 A full load, 400 V input condition, while the proposed structure works at $L_{r2} = 1.1L_{r1}$, $C_{r2} = 1.1C_{r1}$, $L_{m2} = 1.1L_{m1}$, $L_{s12} = 1.2L_{s11}$, $L_{s22} = 1.2L_{s21}$, $L_{s21} = 1.1L_{s11}$, 340 V input voltage, 20 A load. The simulation results are shown in Table V and Fig. 12.

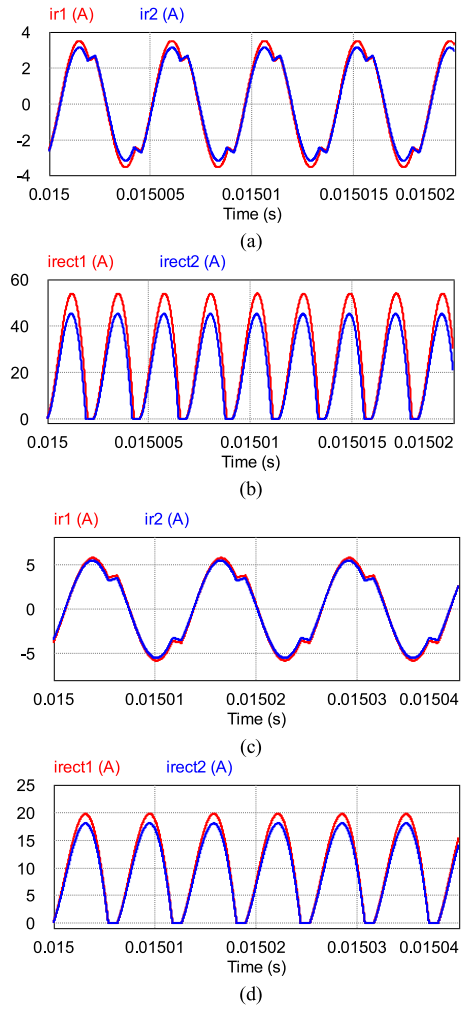

Fig. 11. Simulation waveforms with 5% resonant parameter tolerance: (a) and (b) resonant current and rectifier current of common capacitor structure; (c) and (d) resonant current and rectifier current of the proposed structure.

TABLE V
SIMULATION RESULTS COMPARISON BETWEEN COMMON CAPACITOR STRUCTURE AND THE PROPOSED STRUCTURE WITH 10% RESONANT COMPONENTS TOLERANCES

Result / Structure	i_{r1} (A)	i_{r2} (A)	δi_r (%)
Common capacitor structure	2.66	2.30	7.3
Proposed structure	4.04	3.62	5.5
Result / Structure	i_{rect1} (A)	i_{rect2} (A)	δI_o (%)
Common capacitor structure	31.23	19.68	22.5
Proposed structure	10.69	8.91	9.1

In simulation results of #2, the degree of asymmetry of transformer's secondary windings of the proposed topology structure is 20%. With 10% resonant component parameter tolerances on both the common capacitor structure and the proposed structure, the resonant current sharing error is 7.3% and 5.5%, and the

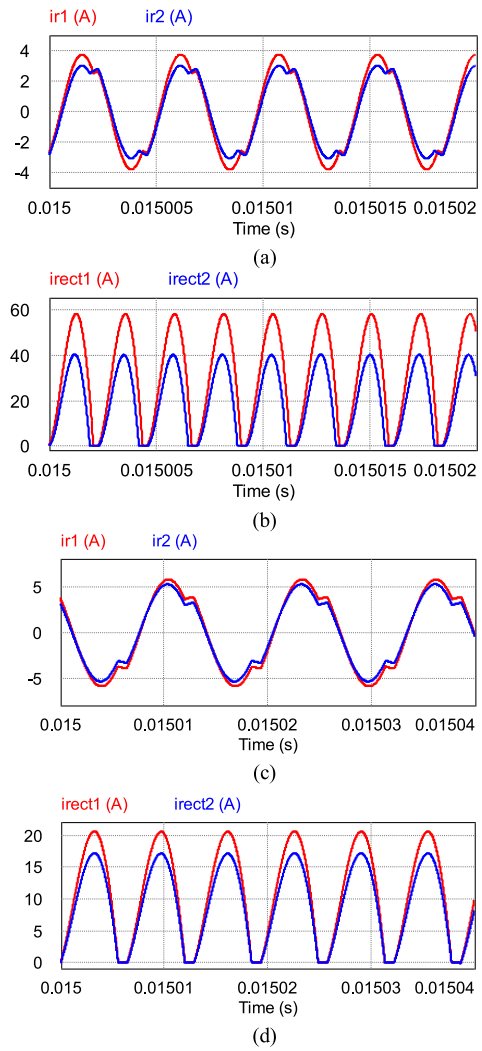

Fig. 12. Waveforms with 10% resonant parameter tolerances: (a) and (b) resonant current and rectifier current of common capacitor structure; (c) and (d) resonant current and rectifier current of the proposed structure.

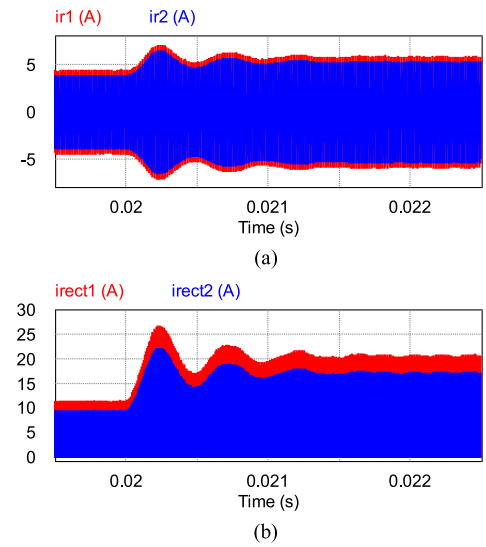

Fig. 13. Simulation waveforms of load transient of proposed structure: (a) resonant currents and (b) rectifier currents.

TABLE VI
PROPOSED STRUCTURE PROTOTYPE PARAMETERS

Input voltage range	340-400 V
Resonant capacitor	Phase1(C_{r1}): 65.7 nF Phase2(C_{r2}): 73.4 nF(1.1C_{r1})
Resonant inductor	Phase1(L_{r1}): 40.0 uH Phase2(L_{r2}): 44.2 uH(1.1L_{r1})
Magnetizing inductor	Phase1(L_{m1}): 152.2 uH Phase2(L_{m2}): 166.2 uH(1.1L_{m1})
Transformer turns ratio n	8.33(25:3:3)
Switch MOSFET	2SK3934
Rectifier diode	STPS20H100CT
Output filter capacitor	470 uF 4 pcs
Output voltage V_o	48 V
Total load power P_o	960 W (2 phases)

rectifier current sharing error is 22.5% and 9.1%, respectively. This demonstrates that the proposed structure can maintain current sharing performance with large component tolerance (10%), which is apparently superior to that of the common capacitor structure.

Part 3: To demonstrate the load transient performance of the proposed structure, this part presents the simulation results with a load current switched from 10 to 20 A at $L_{r2} = 1.1L_{r1}, C_{r2} = 1.1C_{r1}$, $L_{m2} = 1.1L_{m1}$, $L_{s12} = 1.2L_{s11}$, $L_{s22} = 1.2L_{s21}$, $L_{s21} = 1.1L_{s11}$, 340 V input voltage condition.

The simulation current waveforms of phase1 and phase2 during load transients are shown in Fig. 13. Instead of running out of control, the currents can maintain the same changing trend. During load transient, the maximum i_{r1} and i_{r2} are 7.13 and 6.53 A, respectively, and the error is 4.4%, which is close to the value during steady state (5.5%). The maximum rectifier currents of i_{rect1} and i_{rect2} are 26.93 and 22.44 A, respectively, and the error is 9.08%, which is also close to the value during the steady state (9.1%). To sum up, it is demonstrated by the simulation results that during load transients, the current sharing performance can be well maintained.

IV. EXPERIMENTAL RESULTS

A. Verify Current Sharing Performance of the Proposed Structure

To further verify the current sharing performance of the proposed method, a 960-W two-phase LLC resonant converter prototype was built and tested in this section. The detailed prototype parameters are listed in Table VI.

TABLE VII
TEST RESULTS OF THE PROPOSED TOPOLOGY STRUCTURE PROTOTYPE

Result / Input / Load	Resonant currents (rms)			Rectifier currents (avg)		
	i_{r1} (A)	i_{r2} (A)	δI_r (%)	i_{rect1} (A)	i_{rect2} (A)	δI_o (%)
340 V input 240 W load	2.25	1.96	6.9	2.54	2.45	1.8
340 V input 960 W load	4.03	3.55	6.3	10.60	10.20	1.9
400 V input 240 W load	1.74	1.54	6.1	2.49	2.23	5.5
400 V input 960 W load	3.45	3.13	4.9	10.10	10.00	0.5

The secondary windings N_{s11} and N_{s12} are twisted together, as are the windings N_{s21}, N_{s22} to reduce the secondary asymmetry of phase1 and phase2. Since the asymmetry is very small, it is hard to accurately quantify the asymmetries between the secondary sides of the two phases. Instead, the self-inductances of N_{s11}, N_{s1}, N_{s21}, and N_{s22} are easier to measure, which are 2.69 uH, 2.65 uH, 2.83 uH, and 2.89 uH, respectively, and can roughly reflect the asymmetry of secondary sides.

As mentioned in Section II-B, the leakage inductances on the transformer primary side of phase1 (18.8 uH) and phase2 (18.2 uH) are included in the resonant inductances L_{r1} and L_{r2}, respectively. Besides, for the experimental prototype, L_{r1} and L_{r2} also includes extra added discrete inductance L_{r11} (21.2 uH) and L_{r21} (26 uH), respectively, as shown in Fig. 19. L_{r11} and L_{r21} are added in order to acquire the required resonant inductances L_{r1} (40 uH) and L_{r2} (44.2 uH). However, the magnetizing inductances L_{m1} and L_{m2} are provided completely by the transformers, without extra added inductance.

The test data are shown in Table VII, and the test waveforms are shown in Figs. 14–17.

Fig. 14 shows the experimental current waveforms at 340 V input voltage and 240 W load. The switching frequency is 83.7 kHz. Fig. 15 presents the experimental current waveforms at 340 V input voltage and 960 W load, where the switching frequency is 80.2 kHz. And with an input voltage of 400 V, the experimental current waveforms under conditions of 112.7 kHz switching frequency and 240 W load, 104.8 kHz switching frequency and 960 W load are shown in Figs. 16 and 17, respectively.

As shown in Table VII that, with a 340 V input voltage, the resonant current sharing errors are 6.9% and 6.3%, the rectifier current sharing errors are 1.8% and 1.9% at 240 and 960 W load, respectively. While the input voltage is 400 V, the resonant current sharing errors are 6.1% and 4.9%, the rectifier current sharing errors are 5.5% and 0.5% at 240 and 960 W load, respectively.

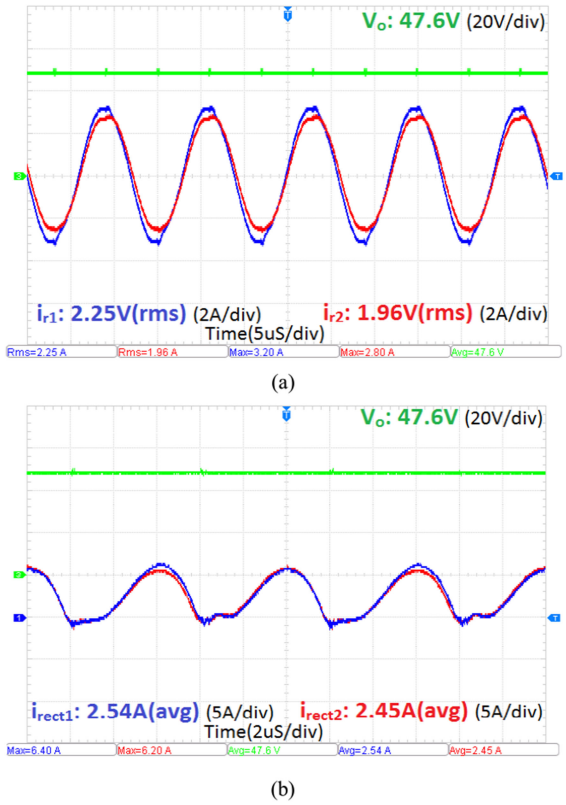

Fig. 14. Experimental waveforms with 340 V input voltage, 240 W load: (a) resonant currents and (b) rectifier currents.

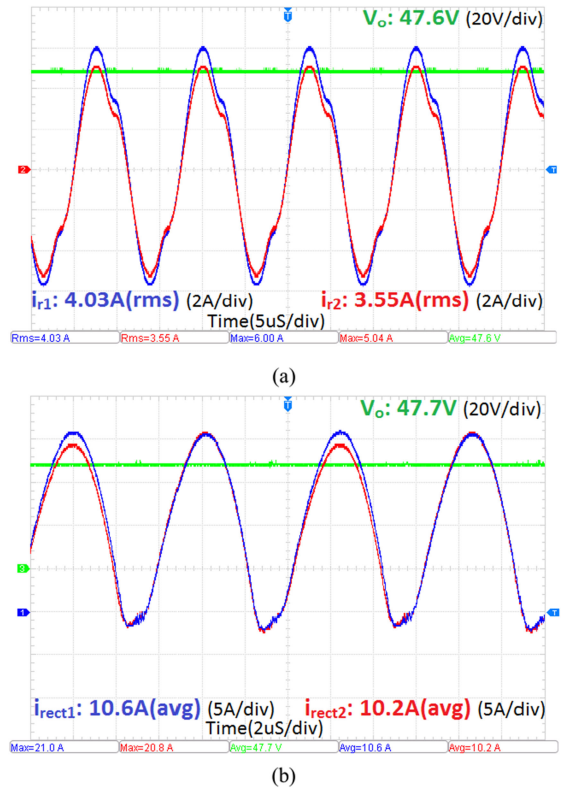

Fig. 15. Experimental waveforms with 340 V input voltage, 960 W load: (a) resonant currents and (b) rectifier currents.

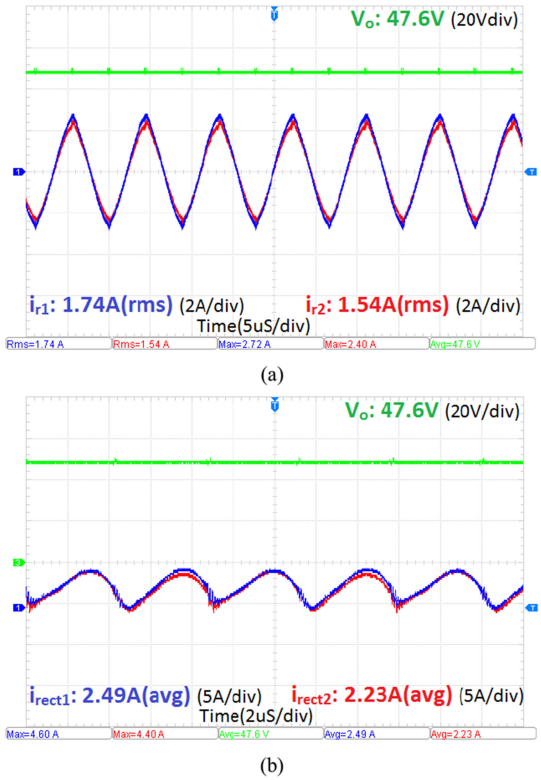

Fig. 16. Experimental waveforms with 400 V input voltage, 240 W load: (a) resonant currents and (b) rectifier currents.

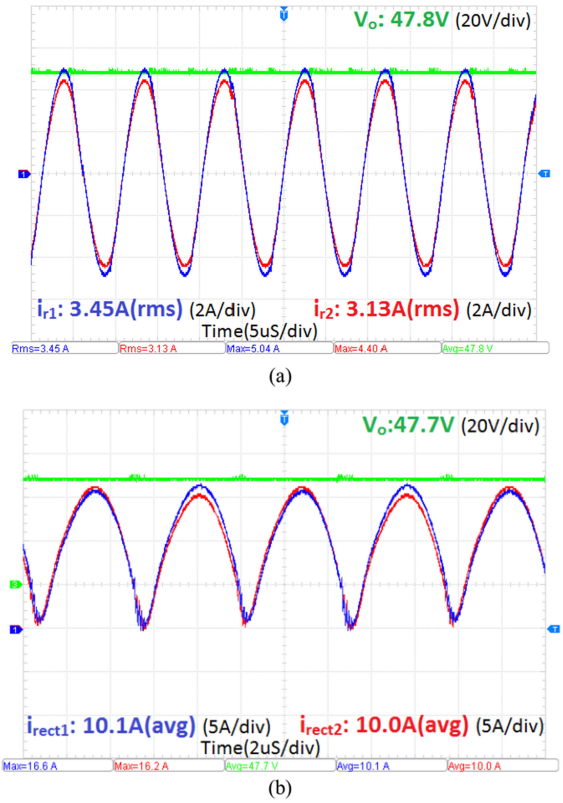

Fig. 17. Experimental waveforms with 400 V input voltage, 960 W load: (a) resonant currents and (b) rectifier currents.

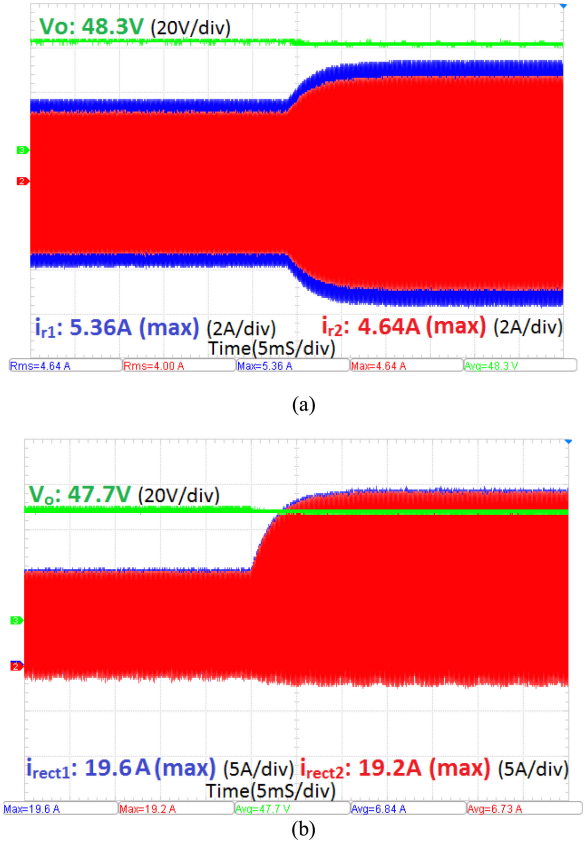

Fig. 18. Load transient waveforms: (a) resonant currents and (b) rectifier currents.

According to the experimental test results shown above, with a component tolerance of 10%, both the resonant currents and rectifier currents are well shared within the whole input voltage and load range. The test results validate the current sharing performance of the proposed structure.

Load transient capability is critical to the automatic current sharing method. The load transient performance of the prototype is tested in the following part, with no current control loop. The input voltage is 340 V, and the load current transfers from 10 A load to 20 A. The experimental results are shown in Fig. 18.

Fig. 18(a) shows that during load transient, the resonant current changing trends of phase1 and phase2 keep consistent with each other. The maximum resonant currents of phase1 and phase2 are 5.36 and 4.64 A, respectively, which reflects that the resonant currents can maintain balance during load transient. Fig. 18(b) shows that the rectifier currents of phase1 and phase2 change in a consistent step with each other during load transient, and the maximum rectifier currents of phase1 and phase2 are 19.6 and 19.2 A, respectively, which keeps the load current sharing performance during load transient. In brief, the load transient test demonstrates the current sharing capability of the proposed multiphase LLC resonant converter during load transient.

Fig. 19 is a test setup picture of the prototype with proposed structure. In the picture T_{r1} and T_{r2} are the transformers of phase1 and phase2, and L_{r11} and L_{r21} are extra added discrete resonant inductances.

Fig. 19. Test setup picture of prototype with proposed structure.

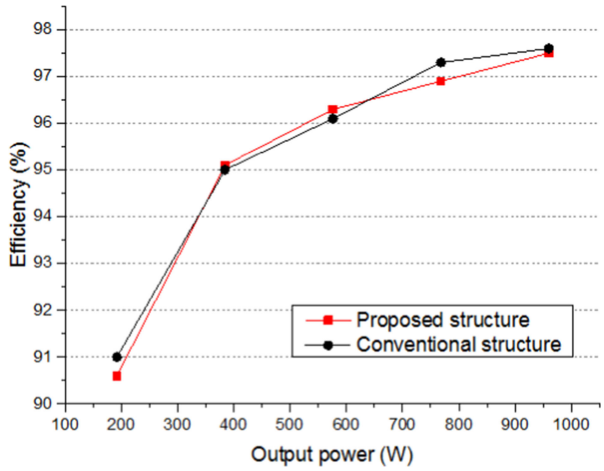

Fig. 20. Efficiency curve of the proposed structure prototype and the conventional structure prototype.

TABLE VIII
PARAMETERS OF THE CONVENTIONAL STRUCTURE PROTOTYPE

Resonant capacitor	Phase1(C_{r1}): 65.7 nF Phase2(C_{r2}): 66.2 nF
Resonant inductor	Phase1(L_{r1}): 35.5 uH Phase2(L_{r2}): 35.8 uH Ferrite Core : EE40 PC40 Copper wire: Φ0.1 mm 80 x strands
Transformer	Turn ratio: 25:6 Magnetizing inductance: Phase1(L_{m1}): 153.1 uH Phase2(L_{m2}): 152.6 uH Ferrite core : EE40 PC40 Copper wire: primary: Φ0.1 mm x 80 strands secondary:Φ0.1 mm 250 strands

B. Verify the Efficiency Performance of the Proposed Structure

To verify the efficiency performance of the proposed structure, an efficiency comparison between the proposed two-phase LLC resonant converter prototype and the conventional two-phase LLC resonant converter prototype is provided as follows.

The parameters of the conventional structure prototype are shown in Table VIII. All parameters of the conventional structure prototype are close to those of the proposed structure prototype, except for the transformer turns ratio. The parameters of each phase in the conventional prototype are basically balanced, ensuring normal operation and balanced currents.

The efficiency curve is shown as Fig. 20. With 100% load, the efficiency of the conventional structure is 97.6%, while it is 97.5% in the proposed structure. With 80% load, the efficiency of the conventional structure is 97.3%, while it is 96.9% in the proposed structure. With 60% load, the efficiency of the conventional structure is 96.1%, while it is 96.3% in the proposed structure. The efficiency comparison indicates that the proposed structure barely impacts the efficiency.

V. CONCLUSION

This article proposed a new current sharing method for multiphase LLC resonant converters by grouping transformers' secondary windings. The proposed method can achieve good current sharing performance even when the components have 10% tolerance. Besides, the proposed method is very simple to realize with neither additional components nor control strategies. What is more, the proposed method would not change the inherent good features of the LLC resonant converter, such as efficiency character and load transient performance. The mathematical analysis provides theoretical supports to the current sharing capability of the proposed multiphase LLC resonant converter, which is validated via PSIM simulation results. With 10% parameter tolerances, the experimental results of 6.9% resonant current sharing error and 5.5% rectifier current sharing error of a 960-W two-phase prototype further verified the current sharing performance of the proposed method. The current sharing performance during load transients and the efficiency performance are also validated by experimental results.

REFERENCES

[1] B. Yang, F. C. Lee, A. J. Zhang, and G. Huang, "LLC resonant converter for front end DC/DC conversion," in *Proc. Appl. Power Electron. Conf. Expo.*, 2002, vol. 2, pp. 1108–1112.

[2] Y. Zhang, D. Xu, M. Chen, Y. Han, and Z. Du, "LLC resonant converter for 48V to 0.9V VRM," in *Proc. 2004 IEEE 35th Annu. Power Electron. Spec. Conf.*, vol. 3, pp. 1848–1854.

[3] T. Jiang, Q. Lin, J. Zhang and Y. Wang, "A novel ZVS and ZCS three-port LLC resonant converter for renewable energy systems," in *Proc. Energy Convers. Congress Expo. (ECCE)*, Sep. 2014, pp. 2296–2302.

[4] S. Zong, H. Luo, W. Li, Y. Deng, and X. He, "Asymmetrical duty cycle-controlled LLC resonant converter with equivalent switching frequency doubler," *IEEE Trans. Power Electron.*, vol. 31, no. 7, pp. 4693–4973, Jul. 2016.

[5] K. Murata and F. Kurokawa, "Performance characteristic of interleaved LLC resonant converter with phase shift modulation," in *Proc. 2015 IEEE Int. Telecommun. Energy Conf. (INTELEC)*, Osaka, 2015, pp. 1–5.
[6] Taotao Jin and Keyue Smedley, "Multiphase LLC series resonant converter for microprocessor voltage regulation," in *Proc. IEEE Industry Appl. Conf. (41st IAS Annu. Meeting)*, 2006, pp. 2136–2143.
[7] B.-C. Kim, K.-B. Park, C.-E. Kim, and G.-W. Moon, "Load sharing characteristic of two-phase interleaved LLC resonant converter with parallel and series input structure," in *Proc. Energy Convers. Congr. Expo.*, 2009, pp. 750–753.
[8] Z. Hu, Y. Qiu, Y.-F. Liu, and P. C. Sen, "An interleaving and load sharing method for multiphase LLC converters," in *Proc. 2013 Twenty-Eighth Annu. IEEE, Appl. Power Electron. Conf. Expo. (APEC)*, pp. 1421–1428.
[9] H. Figge, T. Grote, N. Froehleke, J. Boecker, and P. Ide, "Paralleling of LLC resonant converters using frequency controlled current balancing," in *Proc. 2008. PESC, IEEE Power Electron. Specialists Conf.*, pp. 1080–1085.
[10] Z. Hu, Y. Qiu, Y. Liu, and P. C. Sen, "A control strategy and design method for interleaved LLC converters operating at variable switching frequency," *IEEE Trans. Power Electron.*, vol. 29, no. 8, pp. 4426–4437, Aug. 2014.
[11] K. Murata and F. Kurokawa, "An interleaved PFM LLC resonant converter with phase-shift compensation," *IEEE Trans. Power Electron.*, vol. 31, no. 3, pp. 2264–2272, Mar. 2016.
[12] E. Orietti, P. Mattavelli, G. Spiazzi, C. Adragna, and G. Gattavari, "Current sharing in three-phase LLC interleaved resonant converter," in *Proc. 2009 IEEE Energy Convers. Congress Expo.*, San Jose, CA, pp. 1145–1152.
[13] Y. Hu, A. Amara, and A. Ioinovici, "LLC resonant converter operated at constant switching frequency and controlled by means of a switched-capacitor circuit," *Proc. 2013 1st Int. Future Energy Electron. Conf. (IFEEC)*, Tainan, pp. 691–696.
[14] E. Orietti, P. Mattavelli, G. Spiazzi, C. Adragna, and G. Gattavari, "Two-phase interleaved LLC resonant converter with current-controlled inductor," in *Proc. 2009 Brazilian Power Electron. Conf., Bonito-Mato Grosso do Sul*, pp. 298–304.
[15] B. Kim, K. Park, C. Kim, and G. Moon, "Load sharing characteristic of two-phase interleaved LLC resonant converter with parallel and series input structure," in *Proc. 2009 IEEE Energy Convers. Congress Expo.*, San Jose, CA, pp. 750–753.
[16] H. Wang, Y. Chen, Y. Liu, J. Afsharian, and Z. Yang, "A passive current sharing method with common inductor multiphase LLC resonant converter," *IEEE Trans. Power Electron.*, vol. 32, no. 9, pp. 6994–7010, Sep. 2017.
[17] H. Wang *et al.*, "A common capacitor multi-phase LLC resonant converter," in *Proc. 2016 IEEE Appl. Power Electron. Conf. Expo. (APEC)*, pp. 2320–2327.
[18] H. Wang, Y. Chen, and Y. Liu, "A passive-impedance-matching technology to achieve automatic current sharing for a multiphase resonant converter," *IEEE Trans. Power Electron.*, vol. 32, no. 12, pp. 9191–9209, Dec. 2017.
[19] H. Wang *et al.*, "Common capacitor multiphase LLC converter with passive current sharing ability," *IEEE Trans. Power Electron.*, vol. 33, no. 1, pp. 370–387, Jan. 2018.
[20] K. Yu, J. Du, and H. Ma, "A novel current sharing method for multi-module LLC resonant converters," in *Proc. IECON 2017 – 43rd Annu. Conf. IEEE Ind. Electron. Soc.*, Beijing, pp. 613–618.
[21] Y. Yang, H. Li, H. Miao, W. Huang, and X. Sun, "Design of "EIE" SHAPE coupling inductors and its application in interleaved LLC resonant converter," in *Proc. 2018 IEEE Int. Power Electron. Appl. Conf. Expo. (PEAC)*, Shenzhen, China, pp. 1–5.
[22] B. R. Lin, P. L. Chen, and C. L. Huang, "Analysis of LLC converter with series-parallel connection," in *Proc. 2010 5th IEEE Conf. Ind. Electron. Appl.*, Taichung, pp. 346–351.
[23] B. Lin and J. Dong, "ZVS resonant converter with parallel–series transformer connection," *IEEE Trans. Ind. Electron.*, vol. 58, no. 7, pp. 2972–2979, Jul. 2011.
[24] C. Chien, Y. Wang, and B. Lin, "Analysis of a novel resonant converter with series connected transformers," *IET Power Electron.*, vol. 6, no. 3, pp. 611–623, Mar. 2013.
[25] R. Asensi, R. Prieto, J. A. Cobos, and J. Uceda, "Modeling high-frequency multiwinding magnetic components using finite-element analysis," *IEEE Trans. Magn.*, vol. 43, no. 10, pp. 3840–3850, Oct. 2007.
[26] H. Y. Lu, J. G. Zhu, and S. Y. R. Hui, "Experimental determination of stray capacitances in high frequency transformers," *IEEE Trans. Power Electron.*, vol. 18, no. 5, pp. 1105–1112, Sep. 2003.
[27] C. Liu, L. Qi, X. Cui, and X. Wei, "A terminal capacitance method for analyzing global capacitive effects of magnetic components," *IEEE Trans. Electromagn. Compat.*, vol. 59, no. 4, pp. 1161–1170, Aug. 2017.
[28] F. A. Holguín, R. Asensi, R. Prieto, and J. A. Cobos, "A simplified capacitive model for center-tapped multi-windings transformers," in *Proc. 2015 IEEE Appl. Power Electron. Conf. Expo. (APEC)*, Charlotte, NC, pp. 2504–2511.

Yugang Yang (M'14–SM'18) received the B.S. and M.S. degrees in electrical engineering from Fuxin Mining College, Fuxin, China, in 1989 and 1993, respectively, and the Ph.D. degree in electrical engineering from Tsinghua University, Beijing, China, in 1997. He was a Senior Engineer in power electronics with Huawei Company, Shenzhen, China, from 1998 to 2001. In 2004, he was a Visiting Scholar with the Technical University of Clausthal, Clausthal, Germany, Virginia Polytechnic Instituteand State University, Blacksburg, VA, USA, from 2006 to 2007, and Florida State University, Tallahassee, FL, USA, in 2013. Since 2001, he has been teaching and conducting research on magnetic components and their integration in power electronics converters with Liaoning Technical University, Huludao, China, where he is currently a Professor.

His current research interests include magnetic integration in power electronics converters and bidirectional dc/dc converters.

Junyou Yao was born in Ganzhou, Jiangxi, China. He received the B.S. degree in Nanchang Hangkong University, Nanchang, China, in 2006. He was a Hardware Engineer in power electronics from 2006 to 2017. He is working toward the M.S. degree in electrical engineering from Liaoning Technical University, Huludao, China, since 2017.

His current research interests include power electronics topologies and their magnetic integration technique.

Heng Li was born in Zhoukou, Henan, China. He received the B.S. degree in Liaoning Technical University, Huludao, China, in 2017. He is working toward the M.S. degree in electrical engineering from Liaoning Technical University, Huludao, since 2017.

His current research interests include magnetic integration in power electronics converters and control strategies of power converters.

Jinsheng Zhao was born in Zhoukou, Henan, China. He received the B.S. degree in Liaoning Technical University, Huludao, China, in 2017. He is working toward the M.S. degree in electrical engineering from Liaoning Technical University, Huludao, since 2017.

His current research interests include power electronics topologies and their magnetic integration technique.